IAES International Journal of Artificial Intelligence (IJ-AI)
Vol. 15, No. 1, February 2026, pp. 429~442
ISSN: 2252-8938, DOI: 10.11591/ijai.v15.i1.pp429-442

Brain tumor segmentation and classification using artificial hummingbird optimization algorithm

Radhakrishnan Karthikeyan, Arappaleeswaran Muruganandham
Department of Electronics and Communication Engineering, Rajarajeswari College of Engineering, Bangalore, India

Article Info

Article history:

Received Apr 18, 2024
Revised Nov 10, 2025
Accepted Dec 15, 2025

Keywords:

Adaptive self-guided filtering
Adversarial network
Artificial hummingbird
Brain tumor detection
Dual tree complex discrete wavelet transform
Fuzzy possibilistic C-ordered

ABSTRACT

The time and medical personnel experience are the only factors that determine whether brain tumors can be manually identified from numerous magnetic resonance imaging (MRI) pictures in medical practice. Many frameworks based on brain tumors are diagnosed using both deep learning and machine learning. This study proposes a Wasserstein deep convolutional generative adversarial network (WDCGAN) optimized using the artificial hummingbird optimization algorithm (AHBOA) for brain tumor segmentation and classification (SCBT). First, the BraTS dataset is used to gather the input data. Then it is pre-processed consuming adaptive self-guided filtering (ASGF) and the result is segmented using fuzzy possibilistic C-ordered mean clustering (FPCOMC). After that, features are extracted using the dual tree complex discrete wavelet transform (DT-CDWT). The characteristics of feature extracted are fed to WDCGAN for effectively categorize the various parameters. Then the proposed MATLAB is used to implement the technique, and the performance measurements like F1-score, accuracy, error rate, precision, sensitivity, mean square error, receiver operating characteristic (ROC), and computational time are analyzed. The WDCGAN-AHBOA-SCBT method significantly improves precision in SCBT by integrating adaptive optimization strategies, resulting in 32.18, 32.75, and 32.90% higher precision in contrast to current techniques. This demonstrates that the approach is more accurate and effective, making it a reliable tool for medical diagnosis.

Corresponding Author:

Arappaleeswaran Muruganandham
Department of Electronics and Communication Engineering, Rajarajeswari College of Engineering
Bangalore, India
Email: a.muruganandham@gmail.com

1. INTRODUCTION

Among the most horrifying illnesses of the modern day is brain tumor. The most common reasons are the aberrant cells collective behavior in the brain [1]. In biology, a benign tumor is small and tiny in early stages [2]. When a tumor is considered benign in biology as it is small in the initial stage [3]. When a tumor reaches the secondary stage, it is referred to as malignant since it has grown beyond benign boundaries and is greater in size [4]. About 700,000 people in the USA suffer from brain tumor disease, according to the National Brain Tumor Society [5]. Of those, 30.2% are malignant in origin, and the remaining 69.8% are benign [6]. The report states that only 36% of the patients will survive [7]. About 87,000 in 2020, individuals were diagnosed with brain tumors [8]. There were 84,170 people with brain tumors in 2021, according to estimate [9]. There were 69,950 persons over 40 with a diagnosis. Brain tumors are classified into two stages: high-grade glioma (HGG) and low-grade glioma (LGG) based on their high mortality rate. In addition,

compared to HGG, the LGG survival rate is quicker [10]. Since the average lifespan of HGG is only two years, prompt treatment is necessary.

In the clinics, various methods are employed to treat brain tumors [11]. Radiation therapy is helpful in the benign stage, and surgery is not necessary for the patient to survive [12]. Conversely, the malignant stage is dangerous and is curable with radiation and chemotherapy [13]. As a result, benign tumors usually spread more slowly than malignant ones. But regardless of the situation, diagnosis is critical and requires qualified radiologists [14]. In medical imaging, more contemporary imaging technology has demonstrated remarkable success in the diagnosis and detection of serious human diseases, counting blood cancer, lung cancer, stomach cancer, brain tumors, and a host of other conditions [15]. Computed tomography (CT) and magnetic resonance imaging (MRI) scans are more helpful imaging methods for brain tumors. MRI scans outperforms better than CT imaging when it comes to learn about the texture and tumor shapes. For the purpose of illness prevention and treatment, early identification of brain cancer is crucial. Several deep learning methods are proposed to detect brain tumors. However, the current approach to brain cancer detection is not accurate enough and takes longer to compute. A number of current techniques are offered to address this problem while classifying brain tumors. However, the current method increases calculation time during job execution while providing insufficient precision. The approach of the current methods inspired this development [16]–[21].

Brain tumors are among the most alarming illnesses faced by individuals today, defined by the aggregate actions of aberrant brain cells. Cancer container is classified into benign and malignant categories. Initially, a tumor is termed benign when it is small and confined to its original location. However, as it progresses to a malignant stage, it surpasses its benign boundaries and becomes more threatening. HGG is significantly deadlier, with an average life span of only two years after diagnosis, underscoring the urgency of medical intervention. Brain tumors are treated in various ways; benign tumors usually require radiation therapy without requiring undergoing surgery, whereas malignant or cancerous tumor needs a combination of radiation and chemotherapy. The MRI and CT scan machineries introduced into contemporary medical imaging have played an important part in the identification and diagnosis of severe diseases in humans, such as brain tumors. MRI is exceptionally good at distinguishing the texture and shape of the tumor and is thus extremely valuable for early cancer detection and intervention. Many deep learning frameworks are planned for contribution to brain cancer identification with an aim for high accuracy and low computation time. In general, existing methods seem to be faulty, leading to higher calculation times and unsatisfactory precision during execution.

Although previous works have presented how deep learning influences identifying brain tumors, they have not explicitly addressed how the optimization algorithms influence enhancing the classification accuracy. Most of the existing frameworks are based on conventional machine learning models that often lack the precision required for accurate diagnosis. Additionally, current methods tend to increase computation time and require significant manual intervention. Also, the existing methods identifies the specific tumors to predict and need more algorithms are needed to calculate the different parameters to finalize.

To address these gaps, we propose the Wasserstein deep convolutional generative adversarial network (WDCGAN) optimized through artificial hummingbird optimization algorithm (AHBOA) for brain tumor segmentation and classification (SCBT). This research aims to improve brain tumor classification accuracy by incorporating cutting-edge machine learning methods with optimization strategies. The following are this study's primary contributions:

i) Pre-processing: input images from the BraTS dataset are initially pre-processed using adaptive self-guided filtering (ASGF) to correct corrupted and blurred images.
ii) Segmentation: fuzzy possibilistic C-ordered mean clustering (FPCOMC) segments the affected areas from noise-removed images, preparing them for the subsequent stages.
iii) Feature extraction: dual tree complex discrete wavelet transform (DT-CDWT) extracts Haralick texture features and grayscale statistical features are examples of radiomic features, from the segmented images.
iv) Classification: using the WDCGAN, the processed images are categorized into groups like glioma, meningioma, pituitary, and no tumor.
v) Optimization: AHBOA is utilized to maximize WDCGAN's weight parameters, ensuring accurate brain tumor classification.

2. LITERATURE REVIEW

The literature on the subdivision and classification of brain tumors using deep learning was full of study information; some current attempts were included here. Agrawal *et al.* [16] have suggested that 3D-UNet deep neural networks (DNN) perform brain tumor classification and segmentation. The

pre-processing module takes the pre-processed images first. The distorted and fuzzy images are filtered by the module under presentation. The presented architecture consisted of a better convolutional neural network (CNN) to classify MRI images and a better 3D-UNet prototype for segmenting volumes in the development of an objective expert system to predict brain tumors early.

Devi *et al.* [17] have presented brain tumors are classified and segmented using adaptive kernel fuzzy C means clustering with immobile transmission of wavelet packets that use hybrid deep learning. It is a deep learning system hybrid that is used to diagnose and classify brain tumors. The images which had been processed before were taken advantage of by the feature extraction process. A combination of hybrid adaptive black widow optimization with moth flame optimization (HABWMFO) was used to select the best characteristics. To perform dissection, the adaptive kernel fuzzy C means clustering technique was adjusted.

Preethi and Aishwarya [18] have presented an effective wavelet-fusion image fusion technique of MRI images and positron emission tomography (PET) images of the segmentation and detection of brain tumors. The proposed research presents an efficient fusion-based method of classifying and detecting brain tumors. This is done by first fusing the input image with the help of discrete wavelet transform and a special fusion rule. The fusion process retrieved the features of the gray-level co-occurrence matrix (GLCM). Then demonstrate the brain images as normal or abnormal with an ideal DNN.

Kumar and Karibasappa [19] have presented an attitude depend on the dual-tree complex to identify brain tumors Gabor wavelet transformation (DTCGWT) using Hadoop big data analysis along a neural network. In the presented study, brain tumor categorization and segmentation are achieved by the integration of image processing and huge data. The Hadoop system on MATLAB was used for immense data analysis of the brain tumor images. The data from the investigation is broken down using the recently created dual-tree composite Gabor wavelet transform.

Qader *et al.* [20] have accessible a greater deep convolutional neural network (DCNN) detection and categorization utilizing augmented MRI images by employing hybrid optimization strategies. The presented work adopts improved optimization strategies to assure a development in deep convolutional learning. Additionally, Otsu thresholding was rummage-sale to divide the tumor to sections that focus on brain tumor identification. The presentation of the presented technique is assessed through experimentations on 2,073 enhanced MRI images in all.

Vankdothu and Hameed [21] have showed how brain tumors were divided in the magnetic resonance images applying the support vector machine (SVM) and fuzzy classifier in the machine learning. This research paper explored brain tumor segmentation by the use of CT. Whichever preprocessing method one employs, the techniques of feature extraction are revised prior to subjecting the image to classification steps, whether being the classifier used in SVM of the adaptive neuro-fuzzy inference system (ANFIS) or not to determine whether it is abnormal or normal. Table 1 provides an overview of the reviewed approach.

Although previous research has examined how deep learning affects the identification of brain tumors, they have not explicitly addressed the influence of optimization algorithms on enhancing classification accuracy. Many existing frameworks rely on standard machine learning models, which often lack the precision needed for accurate diagnosis. Additionally, current methods tend to increase computation time and require significant manual intervention. To address these gaps, this work is proposed.

Table 1. Overview of the examined methodology

Reference	Methods	Objectives	Gaps
Agrawal *et al.* [16], 2022	CNN	Develop an expert system for early brain tumor prediction, achieve precise segmentation and classification of brain tumors	Limited to the specific structure of 3D-UNet, may require significant computational resources for processing 3D volumes
Devi *et al.* [17], 2022	HABWMFO	Enhance brain tumor categorization and segmentation accuracy, identify optimal features for diagnosis using HABWMFO	Complexity in combining multiple optimization strategies, may not generalize well to different datasets
Preethi and Aishwarya [18], 2021	DNN	Use fusion techniques to improve segmentation and identification, distinguish between normal and abnormal brain images using deep learning	Potential loss of detail during image fusion, limited focus on specific types of brain tumors
Kumar and Karibasappa [19], 2022	DTCGWT	Integrate big data with image processing for accurate categorization, leverage wavelet transforms for enhanced segmentation	Complexity and resource demands of big data processing, limited scalability beyond Hadoop environments
Qader *et al.* [20], 2022	DCNN	Employ hybrid optimization to improve network performance, accurately detect, and categorize brain tumors in MRI images	Dependence on augmented images may limit real-world applicability, requires extensive computational power for deep learning and optimization
Vankdothu and Hameed [21], 2022	SVM-ANFIS	Utilize SVM and fuzzy classifiers for accurate segmentation, determine the abnormality in CT images	Limited accuracy in specific brain tumor types, may not handle noise and artifacts effectively in CT scans

3. METHOD

WDCGAN-AHBOA-SCBT discusses the brain tumor analysis in affected individuals within this section. This model includes four different projected brain tumor conditions: gliomas, meningiomas, pituitaries, and no tumor images. The prototype undergoes initial data collection by brain tumor illnesses before being forwarded for additional processing. These chapters go through four main developments: preprocessing, segmentation, feature extraction, and categorization, in later sectors. Thus, the explanation is presented accordingly, and Figure 1 represents the recommended WDCGAN-AHBOA-SCBT flow.

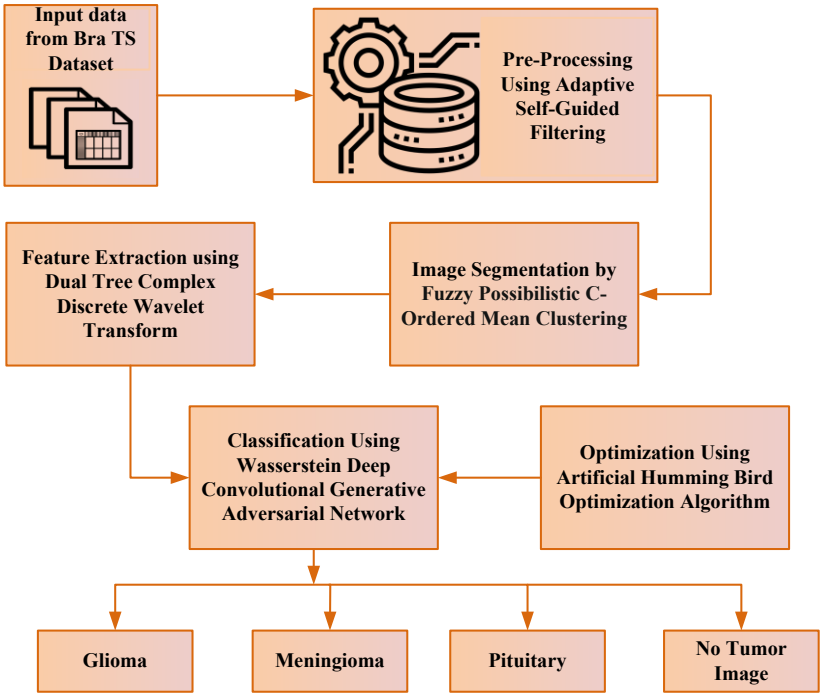

Figure 1. Workflow of the proposed WDCGAN-AHBOA-SCBT framework

3.1. Data acquisition

The data used here is based on BraTS dataset [22]. BraTS have continuously focused on segmenting brain tumors in multimodal MRI data with state-of-the-art methods. BraTS 2020 uses multi-institutional pre-operative MRI imaging for segmenting intrinsically heterogeneous brain tumors, such as gliomas. In order to assess the clinical validity of this segmentation task, evaluate the overall patient's survival, and quantify the tumor's false progression against its actual recurrence, BraTS'20 also uses machine learning algorithms and integrated analyses of radiomics features.

3.2. Adaptive self-guided filtering-based pre-processing

ASGF [23] technique is utilized for pre-processing the brain tumor image. Here, the noises are indifferent from the images while processing the brain tumor images of the crisp edges and it becomes noise-free during the flash/no-flash denoising does the guided filter perform very well in terms of edge preservation. ASGF method is used to adaptively regulate the regularization parameter in each stage of the adaptive guided filtering process of images. Then the regularization is given as (1).

$$p_{n+1}^{i} = \frac{1}{|V|}\sum_{i\in V_l} x_n^l p_n^i + y_n^l \quad (1)$$

Where $n = 0,1,2,\ldots$; p_{n+1}^{i} denoted as the guidance image; $x_n^l p_n^i$ is updated dynamically using the outcomes of each cycle, using the initial guiding image as the input image; V_l denoted as the central pixel of the current window V_n^l, which is l and y_n^l indicates the nth iteration of adaptive guided filtering using input (S_i).

It is crucial to remember that in the current study, this regularization value which is provided by (2) affects whether the window has large variation or is flat.

$$F(x_n^l, y_n^l) = \sum_{i \in V_n^l}((x_n^l p_n^i + y_n^l - S_i)^2 + \varepsilon(x_n^l)^2) \quad (2)$$

Where $n = 1,2,3,\ldots$; ε is the anticipated noise level that determines the regularization parameter; $x_n^l p_n^i$ is updated dynamically using the outcomes of each cycle, using the initial guiding image as the input image; V_l denoted as the central pixel of the current window V_n^l, which is l; y_n^l indicates the n[th] iteration of adaptive guided filtering using input (S_i); and F denotes the regularization parameter of the window's feature. By processing this system, the BraTS dataset's input data is cleansed of image noise. Next, the segmentation phase receives the pre-processed data.

3.3. Segmentation using fuzzy possibilistic C-ordered mean clustering

In this section, FPCOMC [24] method is used for segmenting the affected part from the noise removed image. The ordered method is typical and the flexible possibilistic C-ordered means method that moderates the outlier's effect. Assume that a set of data with M points is divided into the affected part of noise removed images by the FPCOMC algorithm. The following criterion function of FPCOMC is given as (3).

$$\sum_{i=1}^{z} v_{il} = 1 \quad (3)$$

Where v_{il} denotes the k[th] point's membership degree in relation to the i[th] value and $x, y, and\ z$ represented as the parameter of FPCOMC. This comparatively high ranking was supplied by the tumour segmentation in sagittal view pictures. Then the distance which is measured while segmenting is given as (4).

$$T_{il} = \frac{1}{1+\left[\frac{y\beta_{il}}{\delta_i} G_l; u_i\right]} \quad (4)$$

Where δ denoted as the typicality matrix; T_{il} denotes the various factors influence membership and typicality; G_l denotes the distance which is measured using the loss function; β_{il} represents the k[th] point typicality for the i[th] value; and $x, y, and\ z$ represented as the parameter of FPCOMC. The performance of clustering will be impacted by the sensitivity of noise and outliers in the data segmenting the affected part from the noise removed image. Then the affected part of image is given as (5).

$$u_{ik}^{[s]} = \frac{\left[\sum_{l=1}^{n}\left[x(v_{il})^M + \beta_{il} y(T_{il})^\eta\right] F_{ilk}^{[s]} a_{lk}\right]}{\left[\sum_{l=1}^{n}\left[a(v_{il})^M + \beta_{il} y(T_{il})^\eta\right] F_{ilk}^{[s]}\right]} \quad (5)$$

Where T_{il} denotes the various factors influence membership and typicality; $u_{ik}^{[s]}$ is equivalent to the i[th] value center in the s[th] iteration; v_{il} denotes the k[th] point's membership degree in relation to the i[th] value; $F_{ilk}^{[s]}$ represents the parameter that is based on the residual and the loss function; β_{il} represents the k[th] point's typicality for the i[th] cluster; and a_{lk} dependent upon how typical the point is across all values; $x, y, and\ z$ represented as the parameter of FPCOMC. Finally, the affected part images are segmented from the noise removed image, after which the feature extraction section receives the segmented image.

3.4. Feature extraction by dual tree complex discrete wavelet transforms

The segmented affected part pictures are sent to feature extraction and the features are extracted utilizing DT-CDWT [25]. DT-CDWT extracts features accordingly from the segmented images. By utilizing DT-CDWT the grayscale statistic features and features of Haralick texture include mean, skewness, contrast, and homogeneity. The creation of a novel extraction operator employing ridge curve identification is the main objective of the DT-CDWT being presented. In (6) expresses it.

$$e(T) = \sum_{j,l} y_{i,l} v_{j,l}(T) \quad (6)$$

Where j denotes scaling factor that denotes frequencies are inverse; $y_{i,l}$ denoted as set of weighting coefficients; $e(T)$ denotes shift along time axis introduced by the dilation parameter; and $v_{j,l}(T)$ are a collection of fundamental functions that can be acquired by altering a scaling function.

3.4.1. Grayscale statistic features

In this part, the wavelet transform was used to eliminate grayscale statistical characteristics like mean and skewness. Additionally, the following techniques are:

i) Mean: the image's mean color value can be used to define the mean. It expressed in (7).

$$b[N] = (a \times h)[h] \tag{7}$$

Where $j, \mathrm{k}, \mathrm{N}$ denoted as the order of filter; $b[N]$ denoted as the data points of mean image; and $[h]$ denoted as approximation and detail coefficient of mean image.

ii) Skewness: it uses deviation as a measure of the degree of asymmetry in the distribution. In (8) expresses it.

$$b[N] = \sum_{l=-\infty}^{\infty} a\,[l]h[N-l] \tag{8}$$

Where $\mathrm{j}, \mathrm{k}, \mathrm{N}$ denoted as the order of filter; $b[N]$ denoted as the data points of mean image; $[h]$ denoted as approximation and detail coefficient of mean image; and $a[l]$ computed by running it through several segments of image.

3.4.2. Haralick texture features

In this section, the wavelet transform was used to eliminate Haralick texture properties including homogeneity and contrast. Additionally, the following techniques are:

i) Contrast: it calculates the density contrast between a pixel and its surrounding pixels throughout the whole image. In (9) explains the contrast.

$$b_{Low}[N] = \sum_{l=-\infty}^{\infty} a[l]h[2N-l] \tag{9}$$

Where $b_{Low}[N]$ synthesized to low-frequency of DT-CDWT coefficient; j, k, N denoted as the order of filter; $b[N]$ denoted as the data points of mean image; $[h]$ denoted as approximation and detail coefficient of mean image; and $a[l]$ computed by running it through several segments of image.

ii) Homogeneity: it is employed to quantify how close the distribution of GLCM elements is approximated to the GLCM diagonal. In (10) explains the homogeneity.

$$b_{High}[N] = \sum_{l=-\infty}^{\infty} a[l]h[2N-l] \tag{10}$$

Where $b_{High}[N]$ synthesized to high-frequency of DT-CDWT coefficient; $\mathrm{j}, \mathrm{k}, \mathrm{N}$ denoted as the order of filter; $b[N]$ denoted as the data points of mean image; $[h]$ denoted as approximation and detail coefficient of mean image; and $a[l]$ computed by running it through several segments of image.

Finally, grayscale statistical and Haralick texture features are extracted from the images to capture important intensity and texture information. These extracted features are then used as input to the WDCGAN model. Using this approach, the model classifies the images into four categories: glioma, meningioma, pituitary tumor, and no tumor.

3.5. Classification using WDCGAN

WDCGAN [26] is discussed in this section. WDCGAN generates to create a new data by randomly adding noise and fitting images to classify the brain tumor. WDCGAN can classify the output type by adding conditional data to the label of the generator. In (11) represents the two components of the WDCGAN's total addition conditional.

$$b_i = \frac{f^{x_i}}{\sum_{i=1}^{Z} f^{x_i}} \tag{11}$$

Where b_i represent the input of WDCGAN and f^{x_i} represent the outputs of WDCGAN. The original images are classified to create the brain tumor images, which is then fed into the WDCGAN classifier and it is given as in (12).

$$K(G) = -F_{a \approx S_\theta}[G(a)] \tag{12}$$

Where $K(G)$ denoted as the transformed images; $[G(a)]$ denoted as the sub sampling layer is to lessen the altered data's variance; and $F_{a \approx S_\theta}$ represents the values of a specific characteristic in a section of the input

layer. The WDCGAN classifier uses the extended data as its input, and to classify directly from the data and it is given as in (13).

$$K(G) = -F_{a \approx S_r}\left[G(a) + E_{a \approx S_\theta}[G(a)]\right] \quad (13)$$

Where $K(G)$ denoted as the transformed images; $[G(a)]$ denoted as the sub sampling layer is to lessen the altered data's variance; $F_{a \approx S_\theta}$ represents the values of a specific characteristic in a section of the input layer; and $E_{a \approx S_\theta}$ denoted as the max-pooling function. The purpose of the subsampling layer is to lessen the variance of the modified data in order to compute the values of a certain images in the section of input layer and combine them together. Then the variance of the modified data is given as in (14).

$$K(B,S) = -log\, S\,(B|S)_{log} \quad (14)$$

Where K_{log} represents the discriminator's output and $Sr(B|S)$ denoted as the generated data and the original data distribution. Finally, WDCGAN classifies brain cancers into four groups: meningioma, pituitary, glioma, and no tumor. Here, the weight and bias b_i parameters of WDCGAN are tuned using AHBOA.

3.6. Optimization for WDCGAN using AHBOA

AHBOA [27] is proposed to enhance the weights of the WDCGAN. The weight parameter b_i of WDCGAN is optimized using the proposed AHBOA. AHBOA is considered the smallest birds in the world, hummingbirds are amazing creatures. Hummingbirds are the most intellectual species on the planet, even humans, if intelligence is determined using brain-to-body ratio.

- Step 1: initialization. AHBOA's first population was created at random. In (15) then derives the initialization.

$$a_i = low + R.(up - low) \quad (15)$$

  Where 'R' denoted as the random vector between [0 and 1]; a_i denotes the i[th] food supply fits into the solution of a particular issue; and $up\ and\ low$ bounds, both upper, lower, for a d-dimensional problem.
- Step 2: random generation. The input weight parameters are generated randomly following initialization using the AHBOA approach.
- Step 3: fitness function. The input weight parameters are generated randomly following initialization using the AHBOA approach.

$$Fitness\ Function = optimizing[b_i] \quad (16)$$

- Step 4: exploration phase. The three flying skills omnidirectional, diagonal and axial flights that are adequately utilized during foraging are represented by a direction switch vector in the AHA method. In d-dimension space, this vector determines whether one or more directions exist. The exploring phase is then given by (17).

$$u_i(T+1) = a_{i,Tar}(T) + x.H.\left(a_i(T) - a_{i,Tar}(T)\right) \quad (17)$$

  Where $a_{i,Tar}(T)$ is where the i[th] hummingbird plans to visit when it comes to finding food; $u_i(T+1)$ is where i[th] food supply at time T; x denoted as the directed factor an is distributed normally according to N(0, 1); and H denoted as the potential food supply has a higher rate of nectar replenishment than the one that exists now.
- Step 5: exploitation phase for optimizing b_i. After visiting its target food source and consuming the nectar from flowers, a hummingbird searches for a new food source rather than going to another. After that, it takes off for a nearby area within its own range, where it might discover a fresh food source or something better than what it now has. In (18) then provides the exploitation phase.

$$u_i(T+1) = a_i(T) + y.H.a_i(T) \quad (18)$$

  Where $u_i(T+1)$ denotes i[th] food supply at time T; x denoted as the directed factor an is distributed normally according to N(0, 1); H denoted as the potential food supply has a higher rate of nectar replenishment than the one that exists now; and y is a territorial component that has a mean of 0 and distributed according to the normal distribution N 0,1.

– Step 6: termination. The weight parameter of generator b_i from attention induced multi head CNN is optimized by utilizing AHBOA; and it will repeat step 3 until it obtains its halting criteria $a = a + 1$. Then WDCGAN-AHBOA-SCBTD method effectively classifies the brain tumor like glioma, meningioma, pituitary, and no tumor.

4. RESULTS AND DISCUSSION

The untried results of wished-for WDCGAN-AHBOA-SCBT are conferred in this sector. The simulation is executed in Python using PC done Intel core i5, 8 GB RAM, 2.50 GHz CPU, Windows 7 utilizing BraTS dataset. Obtained outcome of the proposed WDCGAN-AHBOA-SCBT approach is analyzed with existing 3D-UNet-DNN-SCBT [16], CNN-long short-term memory (LSTM)-SCBT [17], and DNN–SCBT [18] systems. Figure 2 displays output of proposed WDCGAN-AHBOA-SCBT system.

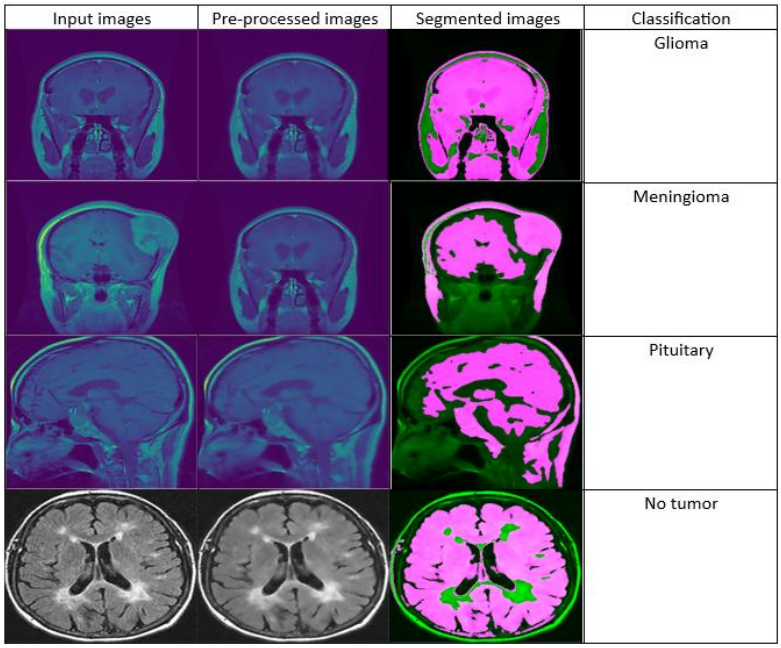

Figure 2. Output result of projected WDCGAN-AHBOA-SCBT method

4.1. Performance measures

The accuracy, precision, and mean square error (MSE) performance measures are used to analyze the desired slant's performance. The following parameters are computed using the suggested approach to obtain the different values, and their significance is emphasized by comparison with the current methods.

– Accuracy: accuracy defines detection rate, which are correctly categorized. Then formula is derived in (19).

$$Accuracy = \frac{(TP+TN)}{(TP+FP+TN+FN)} \tag{19}$$

– Precision: precision computes the count of true positives divided through true positives plus number, false positive number. It is given by (20).

$$Precision = \frac{TP}{(TP+FP)} \tag{20}$$

– MSE: it is measured by MSE, a risk function in statistics. If you wish to penalize huge errors more than little ones in regression and you think your objective is normally distributed, utilize MSE. Then the MSE is derived in (21).

$$\text{MSE} = \frac{1}{n}\sum_{i=1}^{n}\left(Y_i - \hat{Y}_i\right) \tag{21}$$

4.2. Performance analysis

Figures 3 to 5 depicts simulation outcome WDCGAN-AHBOA-SCBT method. The performance metrics are combined with existing 3D-UNet-DNN-SCBT, CNN-LSTM-SCBT, and DNN-SCBT methods. Accuracy analysis is shown in Figure 3. The proposed WDCGAN-AHBOA-SCBT attains 31.82, 32.04, and 32.36% greater accuracy for brain tumor image which is examined compared with existing 3D-UNet-DNN-SCBT, CNN-LSTM-SCBT, and DNN–SCBT methods. Figure 4 depicts the performance analysis of proposed methodology. The proposed WDCGAN-AHBOA-SCBT attains 31.18, 32.75, and 32.90% greater for precision; attains 29.18, 30.51, and 31.75% greater for sensitivity; attains 32.53, 32.71, and 32.81% greater for recall; attains 30.15, 31.50, and 32.91% higher for sensitivity; and attains 28.95, 31.20, and 32.48% higher for F1-score [28] which is analyzed with existing 3D-UNet-DNN-SCBT, CNN-LSTM-SCBT, and DNN–SCBT methods. Analysis of MSE is shown in Figure 5. The proposed WDCGAN-AHBOA-SCBT attains 28.72, 30.94, and 31.04% lower MSE for glioma; attains 29.68, 30.71, and 31.92% lower MSE for meningioma; attains 31.53, 32.83, and 32.11% lower MSE for pituitary; and attains 29.75, 30.80, and 31.15% lower MSE for no tumor image which is analyzed with existing 3D-UNet-DNN-SCBT, CNN-LSTM-SCBT and DNN–SCBT methods.

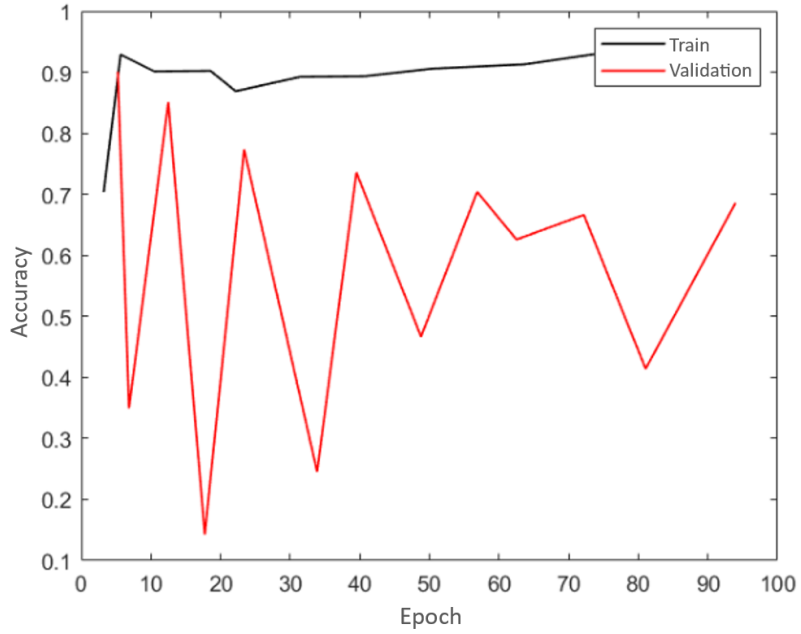

Figure 3. Accuracy analysis

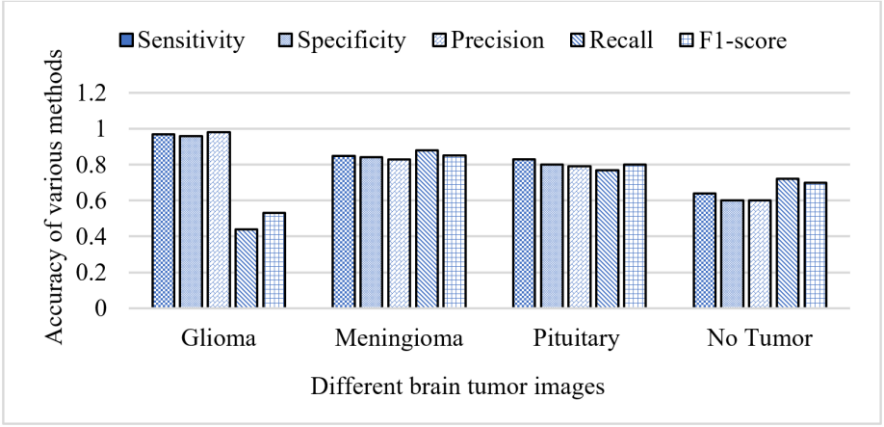

Figure 4. Performance analysis

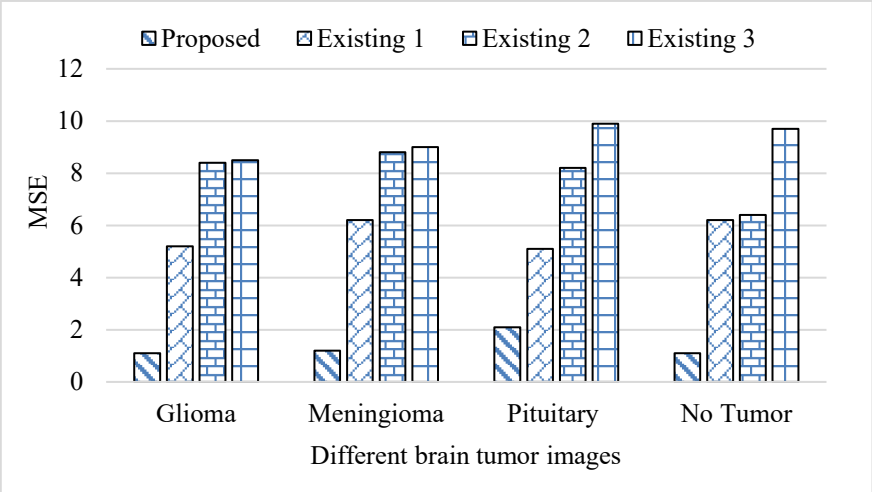

Figure 5. Mean square error analysis

Table 2 presents some comparative analyses done among various methods for segmenting brain tumors and categorization, showing striking variance in certain performance metrics such as accuracy, precision, kappa statistic (Kappa), Matthew correlation coefficient (MCC), average Hausdorff distance (AHD), processing time, error rate, intersection over union (IoU), dice similarity coefficient, specificity score, and Hausdorff distance. The CNN approach had an accuracy of 89.57% with precision at 90.86% and a Kappa value of 90.45, depicting good performance but with relatively high processing time at 0.7 and an error rate of 0.6. Among them, the HABWMFO method had a lower accuracy of 78.54% but a very high precision at 89.07%. On the other hand, the DNN approach achieved a higher accuracy of 90.65% at precision 88.96%, reflecting its very strong performance in various metrics such as MCC and IoU.

Table 2. Performance comparison of brain tumor segmentation methods

Methods	Accuracy (%)	Precision (%)	Kappa statistic	MCC	AHD	Processing time	Error rate	IoU	Dice similarity	Specificity score	Hausdorff distance
CNN [16]	89.57	90.86	90.45	88.78	79.56	0.7	0.6	88.95	75.4	65.4	76
HABWMFO [17]	78.54	89.07	88.97	89.47	79.97	0.6	0.4	89.75	58.76	77.976	73
DNN [18]	90.65	88.96	90.52	89.63	90.82	0.5	0.6	89.62	66.57	85.24	77
DTCGWT [19]	90.48	89.74	78.55	89.42	93.51	0.4	0.5	89.72	75.42	65.3	76
DCNN [20]	90.23	89.98	90.53	92.82	90.91	0.6	0.6	92.82	67.82	74.81	69
SVM-ANFIS [21]	90.81	88.62	90.83	89.82	90.79	0.5	0.4	89.72	66.4	85.6	76
WDCGAN-AHBOA-SCBT (proposed)	99.97	98.82	99.82	99.83	99.89	0.1	0.1	99.83	95.82	96.6	25

The SVM-ANFIS demonstrated the effectiveness of the combination of machine learning with fuzzy logic and the accuracy of 90.81% and precision of 88.62%. The proposed approach, WDCGAN-AHBOA-SCBT, was far much better with an accuracy of 99.97%, precision of 98.82%, Kappa of 99.82, and MCC of 99.83 at the expense of all other methods. The approach also presented improved values of AHD, IoU, and dice similarity coefficient with the least values of processing time and error rate at 0.1 and very low Hausdorff distance of 25. It is this in-depth comparison that provides reason to believe that the suggested approach is much superior to the current ones in terms of enhancement of the segmentation and categorization of accuracy, efficiency, and reliability.

Table 3 contrasts the computational cost and complexity of many techniques for segmenting and classifying brain tumors. The computing demands vary for each approach, thus making a big difference in the applicability and performance of an applicable technique. The CNN approach displays a modest efficiency in both computational cost and complexity, with a value of 0.5 and 0.7, respectively. The HABWMFO methodology has a lower level of complexity, standing at 0.6, yet higher on computational cost, standing at 0.7, which means this technique is less complicated than some other techniques but requires more computational resources. The DNN approach is resource-intensive but has a comparatively simpler computational structure, as inferred from its computational cost of 0.7 and complexity of 0.5. The DTCGWT

approach is notable for its resource efficiency but execution complexity, with a lower computational cost of 0.4 yet higher complexity of 0.8.

Table 3. Computational cost and complexity

Methods	Computational cost	Computational complexity
CNN [16]	0.5	0.7
HABWMFO [17]	0.7	0.6
DNN [18]	0.7	0.5
DTCGWT [19]	0.4	0.8
DCNN [20]	0.5	0.8
SVM-ANFIS [21]	0.6	0.7
WDCGAN-AHBOA-SCBT (proposed)	0.001	0.02

Apart from this, with a 0.5 computational cost and 0.8 complexity, the enhanced CNN shows a similar profile, underlining its efficiency of resources with a more complex computational process. SVM-ANFIS depicts a balance between resource and complexity requirements with 0.6 computational cost and 0.7 complexity. On the other hand, for the SCBT, the WDCGAN optimized with AHBOA has only 0.001 and 0.02 for computational cost and complexity, respectively. The significant reduction of these values indicates that the proposed technique is superior; this makes the processing and execution faster, using less resource as compared to other traditional techniques, which make them very much applicable in practical diagnostics.

4.3. Statistical analysis of the proposed method verses existing methods

Three statistical tests are conducted: Friedman test, Wilcoxon signed-rank test (WSR test), and Shapiro-Wilk test (SW test). The SW test is a statistical test used to determine whether a dataset is normally distributed. In actual sense, the null hypothesis tested is that the data come from a normally distributed population. The outcome of the test is a W statistic, along with a p-value. If the p-value is less than the selected significance level of 0.05, under which one assumes the null hypothesis of normality of the data, then the null hypothesis is rejected. WSR test or Mann-Whitney U-test, is a non-parametric statistical test used to compare two related samples or repeated dimensions on the same model to assess whether the mean ranks of their occupant's change. It is used when the data fail to meet the assumptions for the paired t-test, especially in cases of inconsistent distribution of the differences between the pairs. The Kruskal-Wallis (H-test) is a non-parametric statistical test used to associate differences between three or more independent assemblages on a single unremitting or ordinal outcome. This test ranks the data points across the groups collectively and determines if the ranks differ significantly between the groups, extending the Mann-Whitney U-test to multiple groups. This test is useful in cases where the ANOVA assumptions are violated and makes no assumptions of normal distribution of the data. A significant H-test indicates that at least one group is different from the remainder, although the test itself does not establish which groups are different, and therefore requires study through post-hoc testing.

Statistical comparisons between the suggested approach, WDCGAN-AHBOA-SCBT, with current approaches are given in Table 4 using the SW test, WSR test/U-test, H-test, mean, standard deviation, and variance inflation factor. The p values in SW, WSR, and H-test refer to the statistical effect of practical differences among approaches. For instance, the p values obtained in the CNN technique [16] are 0.24, 0.21, and 0.34, respectively, reflecting a moderate degree of statistical significance.

Table 4. Statistical analysis of the proposed method verses existing methods

Methods	SW test p-value	WSR test/ U-test p-value	H-test p-value	Mean	Standard deviation	Variance inflation factor
CNN [16]	0.24	0.21	0.34	59,698.99	1,342.94	1.98
HABWMFO [17]	0.34	0.26	0.374	327,567.07	2,945.03	1.05
DNN [18]	0.374	0.267	0.29	254,375.9	1,244.04	1.76
DTCGWT [19]	0.26	0.35	0.21	59,698.99	1,522.54	1.05
DCNN [20]	0.227	0.44	0.26	357,543.9	3,128.04	1.86
SVM-ANFIS [21]	0.374	0.267	0.267	456,743.9	2,899.67	2.40
WDCGAN-AHBOA-SCBT (proposed)	<0.001	<0.001	<0.001	59,698.99	4,679.66	1.001

In comparison to the suggested technique, the HABWMFO method [17] and DNN method [18] have somewhat higher p-values, indicating a less significant performance difference. The DTCGWT method of [19] has moderate statistical significance with p-values of 0.26, 0.35, and 0.21, while for approaches such as DCNN [20] and SVM-ANFIS [21], the differences are even less statistically significant. On the other hand,

the proposed WDCGAN-AHBOA-SCBT approach, having given p-values less than 0.001 in each test, represents outstanding performance and very high statistical significance compared to existing methods. Its standard deviation is 4,679.66 for the suggested technique, pointing to some unreliability in performance, probably because of its sophisticated algorithmic design that encompasses a large number of instances, although the mean value for most of the methods is around similar values. For the suggested approach, the variance inflation factor is remarkably low at 1.001, indicating negligible multicollinearity and indicating the stability and dependability of the suggested model. Overall, these statistical findings highlight the intended WDCGAN-AHBOA-SCBT method's superiority over conventional approaches in terms of statistical significance, variability handling, and stability.

4.4. Ablation study of the proposed method

Ablation studies are systematic experiments conducted to study the effects of specific elements or characteristics of a proposed approach. An ablation study concerning the WDCGAN-AHBOA-SCBT methodology would involve systematically removing or changing elements or procedures in teaching and observing how they affect the overall performance of the mock-up. Table 5 shows the ablation study of the proposed method against the previously described CNN and generative adversarial network (GAN) networks.

It is observed that the WDCGAN-SCBT approach has significantly improved, yielding an accuracy of 95.12% and recall of 96.52%. However, its precision is 93.15%, while the F1-score is 92.14%, indicating that there is a slight trade-off between precision and the F1-score. Also, the suggested WDCGAN-AHBOA-SCBT technique outperforms all others with an accuracy, precision, recall, and F1-score of 99.89, 99.9, 99.87, and 99.8% respectively. These results justify that AHBOA can be well incorporated for parameter optimization to strengthen the performance for an accurate segmentation and classification of brain tumors. Overall, the proposed approach has achieved much better improvements compared to other state-of-the-art approaches and proves to be an effective and highly efficient method in brain tumor analysis.

Table 5. Ablation study of the proposed method

Methods	BraTS dataset			
Performance metrics	Accuracy (%)	Precision (%)	Recall (%)	F1-score (%)
CNN [29]	90.56	92.87	91.86	94.89
GAN [30]	91.93	93.09	92.86	95.76
WDCGAN-SCBT	95.12	93.15	96.52	92.14
WDCGAN-AHBOA-SCBT (proposed)	99.89	99.9	99.87	99.8

5. CONCLUSION

The overall flow of the proposed methodology is shown in this section. At the very principal, the input data is gathered from BraTS dataset. In order to do that, input data is pre-processed using ASGF, and the pre-processed data is then segmented using FPCOMC. Then the extracted features by DT-CDWT are given as input to WDCGAN for the efficient classification of various parameters. Generally, WDCGAN does not promptly adapt optimization techniques to handle ideal parameters for the exact classification of brain tumors. So, AHBOA will optimize WDCGAN, which rightly classifies glioma, meningioma, pituitary, and no tumor. Then the model generates the segmented image after recovering those losses. Then, the performance of the proposed WDCGAN-AHBOA-SCBT implemented in MATLAB is analyzed with respect to performance metrics such as the F1-score, accuracy, error rate, precision, sensitivity, MSE, receiver operating characteristic (ROC), and computational time. By combining adaptive optimization approaches, the proposed WDCGAN-AHBOA-SCBT method significantly enhances precision in segmenting and categorizing brain tumors, with 32.18, 32.75, and 32.90 higher precision compared to different existing approaches such as 3D-UNet-DNN-SCBT, CNN-LSTM-SCBT, and DNN–SCBT, respectively. This advantage delineates the superior accuracy and efficiency and identifies it as a reliable tool for diagnosing conditions. Further research should be directed at expanding databases to represent a wide range of people, optimizing it for real-time processing in a clinical setting, interfacing it with other diagnostic tools, and developing adaptive learning methodologies. Clinical validation and user feedback will be necessary to develop this model for practical usability in real life and its integration into existing workflows.

ACKNOWLEDGMENTS

The support for this research is provided by the VTU Research Centre, Department of Electronics and Communication Engineering, Rajarajeswari College of Engineering, Bengaluru, India.

FUNDING INFORMATION

Authors state no funding involved.

AUTHOR CONTRIBUTIONS STATEMENT

This journal uses the Contributor Roles Taxonomy (CRediT) to recognize individual author contributions, reduce authorship disputes, and facilitate collaboration

Name of Author	C	M	So	Va	Fo	I	R	D	O	E	Vi	Su	P	Fu
Radhakrishnan Karthikeyan	✓	✓			✓	✓			✓	✓				
Arappaleeswaran Muruganandham		✓			✓	✓			✓	✓				

C : **C**onceptualization
M : **M**ethodology
So : **So**ftware
Va : **Va**lidation
Fo : **Fo**rmal analysis
I : **I**nvestigation
R : **R**esources
D : **D**ata Curation
O : Writing - **O**riginal Draft
E : Writing - Review & **E**diting
Vi : **Vi**sualization
Su : **Su**pervision
P : **P**roject administration
Fu : **Fu**nding acquisition

CONFLICT OF INTEREST STATEMENT

Authors state no conflict of interest.

DATA AVAILABILITY

This paper presents one dataset that have been used and openly available in Kaggle at https://www.kaggle.com/datasets/awsaf49/brats2020-training-data.

REFERENCES

[1] R. Vankdothu, M. A. Hameed, and H. Fatima, "A brain tumor identification and classification using deep learning based on CNN-LSTM method," *Computers and Electrical Engineering*, vol. 101, 2022, doi: 10.1016/j.compeleceng.2022.107960.
[2] N. Noreen, S. Palaniappan, A. Qayyum, I. Ahmad, M. Imran, and M. Shoaib, "A deep learning model based on concatenation approach for the diagnosis of brain tumor," *IEEE Access*, vol. 8, pp. 55135–55144, 2020, doi: 10.1109/ACCESS.2020.2978629.
[3] A. Sekhar, S. Biswas, R. Hazra, A. K. Sunaniya, A. Mukherjee, and L. Yang, "Brain tumor classification using fine-tuned GoogLeNet features and machine learning algorithms: IoMT enabled CAD system," *IEEE Journal of Biomedical and Health Informatics*, vol. 26, no. 3, pp. 983–991, 2022, doi: 10.1109/JBHI.2021.3100758.
[4] S. A. A. Ismael, A. Mohammed, and H. Hefny, "An enhanced deep learning approach for brain cancer MRI images classification using residual networks," *Artificial Intelligence in Medicine*, vol. 102, 2020, doi: 10.1016/j.artmed.2019.101779.
[5] W. Deng, Q. Shi, M. Wang, B. Zheng, and N. Ning, "Deep learning-based HCNN and CRF-RRNN model for brain tumor segmentation," *IEEE Access*, vol. 8, pp. 26665–26675, 2020, doi: 10.1109/ACCESS.2020.2966879.
[6] M. O. Khairandish, M. Sharma, V. Jain, J. M. Chatterjee, and N. Z. Jhanjhi, "A hybrid CNN-SVM threshold segmentation approach for tumor detection and classification of MRI brain images," *Innovation and Research in BioMedical engineering*, vol. 43, no. 4, pp. 290–299, 2022, doi: 10.1016/j.irbm.2021.06.003.
[7] M. A. Naser and M. J. Deen, "Brain tumor segmentation and grading of lower-grade glioma using deep learning in MRI images," *Computers in Biology and Medicine*, vol. 121, 2020, doi: 10.1016/j.compbiomed.2020.103758.
[8] Y. Ding *et al.*, "MVFusFra: a multi-view dynamic fusion framework for multimodal brain tumor segmentation," *IEEE Journal of Biomedical and Health Informatics*, vol. 26, no. 4, pp. 1570–1581, 2022, doi: 10.1109/jbhi.2021.3122328.
[9] M. Humayun, M. I. Khalil, G. Alwakid, and N. Z. Jhanjhi, "Superlative feature selection based image classification using deep learning in medical imaging," *Journal of Healthcare Engineering*, vol. 2022, pp. 1–11, 2022, doi: 10.1155/2022/7028717.
[10] M. Rizwan, A. Shabbir, A. R. Javed, M. Shabbir, T. Baker, and D. Al-Jumeily Obe, "Brain tumor and glioma grade classification using Gaussian convolutional neural network," *IEEE Access*, vol. 10, pp. 29731–29740, 2022, doi: 10.1109/ACCESS.2022.3153108.
[11] M. Aamir *et al.*, "A deep learning approach for brain tumor classification using MRI images," *Computers and Electrical Engineering*, vol. 101, 2022, doi: 10.1016/j.compeleceng.2022.108105.
[12] B. Deepa, M. Murugappan, M. G. Sumithra, M. Mahmud, and M. S. Al-Rakhami, "Pattern descriptors orientation and MAP firefly algorithm based brain pathology classification using hybridized machine learning algorithm," *IEEE Access*, vol. 10, pp. 3848–3863, 2022, doi: 10.1109/ACCESS.2021.3100549.
[13] A. S. Musallam, A. S. Sherif, and M. K. Hussein, "A new convolutional neural network architecture for automatic detection of brain tumors in magnetic resonance imaging images," *IEEE Access*, vol. 10, pp. 2775–2782, 2022, doi: 10.1109/ACCESS.2022.3140289.
[14] J. Zhang, Z. Jiang, J. Dong, Y. Hou, and B. Liu, "Attention gate ResU-Net for automatic MRI brain tumor segmentation," *IEEE Access*, vol. 8, pp. 58533–58545, 2020, doi: 10.1109/ACCESS.2020.2983075.
[15] F. Fang, Y. Yao, T. Zhou, G. Xie, and J. Lu, "Self-supervised multi-modal hybrid fusion network for brain tumor segmentation," *IEEE Journal of Biomedical and Health Informatics*, vol. 26, no. 11, pp. 5310–5320, 2022, doi: 10.1109/jbhi.2021.3109301.
[16] P. Agrawal, N. Katal, and N. Hooda, "Segmentation and classification of brain tumor using 3D-UNet deep neural networks," *International Journal of Cognitive Computing in Engineering*, vol. 3, pp. 199–210, 2022, doi: 10.1016/j.ijcce.2022.11.001.

[17] R. S. Devi, B. Perumal, and M. P. Rajasekaran, "A hybrid deep learning based brain tumor classification and segmentation by stationary wavelet packet transform and adaptive kernel fuzzy c means clustering," *Advances in Engineering Software*, vol. 170, p. 103146, Aug. 2022, doi: 10.1016/j.advengsoft.2022.103146.
[18] S. Preethi and P. Aishwarya, "An efficient wavelet-based image fusion for brain tumor detection and segmentation over PET and MRI image," *Multimedia Tools and Applications*, vol. 80, no. 10, pp. 14789–14806, 2021, doi: 10.1007/s11042-021-10538-3.
[19] S. H. S. Kumar and K. Karibasappa, "An approach for brain tumour detection based on dual-tree complex Gabor wavelet transform and neural network using Hadoop big data analysis," *Multimedia Tools and Applications*, vol. 81, no. 27, pp. 39251–39274, 2022, doi: 10.1007/s11042-022-13016-6.
[20] S. M. Qader, B. A. Hassan, and T. A. Rashid, "An improved deep convolutional neural network by using hybrid optimization algorithms to detect and classify brain tumor using augmented MRI images," *Multimedia Tools and Applications*, vol. 81, no. 30, pp. 44059–44086, 2022, doi: 10.1007/s11042-022-13260-w.
[21] R. Vankdothu and M. A. Hameed, "Brain tumor segmentation of MR images using SVM and fuzzy classifier in machine learning," *Measurement: Sensors*, vol. 24, 2022, doi: 10.1016/j.measen.2022.100440.
[22] R. A. Zeineldin, M. E. Karar, O. Burgert, and F. M.-Ullrich, "Multimodal CNN Networks for Brain Tumor Segmentation in MRI: a BraTS 2022 Challenge Solution," in *Brainlesion: Glioma, Multiple Sclerosis, Stroke and Traumatic Brain Injuries*, 2023, pp. 127–137, doi: 10.1007/978-3-031-33842-7_11.
[23] S. Zhu and Z. Yu, "Self-guided filter for image denoising," *IET Image Processing*, vol. 14, no. 11, pp. 2561–2566, 2020, doi: 10.1049/iet-ipr.2019.1471.
[24] R. J. Kuo, J.-Y. Lin, and T. P. Q. Nguyen, "An application of sine cosine algorithm-based fuzzy possibilistic C-ordered means algorithm to cluster analysis," *Soft Computing*, vol. 25, no. 5, pp. 3469–3484, 2020, doi: 10.1007/s00500-020-05380-y.
[25] R. Sharbati, F. Khoshnoudian, M. Koopialipoor, and M. M. Tahir, "Applying dual-tree complex discrete wavelet transform and Gamma modulating function for simulation of ground motions," *Engineering with Computers*, vol. 37, no. 2, pp. 1519–1535, 2019, doi: 10.1007/s00366-019-00898-8.
[26] J. Li, Z. Chen, L. Cheng, and X. Liu, "Energy data generation with wasserstein deep convolutional generative adversarial networks," *Energy*, vol. 257, 2022, doi: 10.1016/j.energy.2022.124694.
[27] W. Zhao, L. Wang, and S. Mirjalili, "Artificial hummingbird algorithm: a new bio-inspired optimizer with its engineering applications," *Computer Methods in Applied Mechanics and Engineering*, vol. 388, 2022, doi: 10.1016/j.cma.2021.114194.
[28] B. Jaishankar, A. A.M., V. D., and L. Raja, "A novel epilepsy seizure prediction model using deep learning and classification," *Healthcare Analytics*, vol. 4, 2023, doi: 10.1016/j.health.2023.100222.
[29] A. W. Salehi *et al.*, "A study of CNN and transfer learning in medical imaging: advantages, challenges, future scope," *Sustainability*, vol. 15, no. 7, 2023, doi: 10.3390/su15075930.
[30] F. Jiang, J. Ma, C. J. Webster, X. Li, and V. J. L. Gan, "Building layout generation using site-embedded GAN model," *Automation in Construction*, vol. 151, 2023, doi: 10.1016/j.autcon.2023.104888.

BIOGRAPHIES OF AUTHORS

Radhakrishnan Karthikeyan has an impressive academic and professional background. Having received his B.E. degree from Bharathiar University, Coimbatore in 1992 and his M.E. degree from Anna University in 2011, he has demonstrated a commitment to education and personal growth over the years. With over 10 years of experience in teaching, research, and administrative roles across different engineering colleges, autonomous institutions, and universities, he has undoubtedly developed a wealth of knowledge and expertise in his field. His contribution to academia extends beyond the classroom, he has actively contributed to the dissemination of knowledge in his area of specialization, which is image processing. His research interests in image processing indicate a dedication to advancing the understanding and application of this field, which is increasingly important in various domains such as healthcare, surveillance, and multimedia. He can be contacted at email: rkarthi123@gmail.com.

Dr. Arappaleeswaran Muruganandham received the B.E. degree in Electronics and Communication Engineering (1993) and M.E. degree in Communication Systems (2000) from University of Madras and National Institute of Technology (NIT), Trichy respectively. He completed the Ph.D. (Image Processing) degree in Anna University, Chennai in the year 2013. He is a life member of ISTE and FIE member of IEEE. He is currently working as a professor in the Department of Electronics and Communication Engineering, Rajarajeswari College of Engineering, Bengaluru, VTU, Karnataka, India and has a teaching experience of 25 years. His-research interests include signal and image processing and bio medical image processing. He can be contacted at email: a.muruganandham@gmail.com.